Slow Spinodal Decomposition in Binary Liquid Mixtures of Polymers. 2. Effects of Molecular Weight and Transport Mechanism

Mikihito Takenaka, Tatsuo Izumitani,† and Takeji Hashimoto*

Department of Polymer Chemistry, Kyoto University, Kyoto 606, Japan.
Received October 20, 1986

ABSTRACT: The early stage of the spinodal decomposition of binary polymer mixtures of polybutadiene and styrene–butadiene random copolymer (SBR) at a composition of 50/50 w/w was studied by time-resolved light scattering as a function of molecular weight of SBR at 60 °C, which is well above the glass transition temperature of both components; thus, the two components are in the liquid state. The early stage of the spinodal decomposition of the mixtures was found to be described with a good approximation by the linearized theory of Cahn, the analyses of which yielded characteristic parameters for the early stage of the spinodal decomposition. The parameter q_m^2/D_{app} shows the molecular weight dependence of M^1 at the high molecular weight limit, supporting the fact that the decomposition involves mutual diffusion of center of mass of polymer molecules via reptation (q_m is the wavenumber of the dominant mode of the fluctuations, and D_{app} is the mutual diffusivity of the mixture). The large wavelength, $2\pi/q_m$, of the dominant mode of fluctuations relative to the size of the individual molecules was found to be primarily due to the small temperature dependence of the interaction parameter χ between the two polymer which makes $\epsilon = (\chi - \chi_s)/\chi_s$ (χ_s, χ value at spinodal temperature) very small, even though the actual quench depth, $\Delta T = |T_s - T|$, is large (T_s and T, spinodal temperature and phase separation temperature, respectively), e.g., the mixture being effectively close to spinodal point.

I. Introduction

In the previous paper[1] a very slow spinodal decomposition was reported for the binary liquid mixtures of polybutadiene (PB) and styrene–butadiene random copolymer (SBR) at temperatures well above the glass transition temperatures (T_g's) of the constituent polymers. The time scale where the early stage of the spinodal decomposition (SD) can be described with good accuracy by the linearized theory of Cahn[2] was found to extend over more than 1 h at 40 °C, for example, which is due to the system having a very long characteristic time, t_c, as defined by

$$t_c = \xi^2/D_{app} \tag{I-1}$$

where ξ^2 and D_{app} are the thermal correlation length and mutual diffusivity of the mixture at a given temperature, T.

Since the characteristic times of the mixtures are expected to vary very much depending on the systems, it is quite useful to compare the time evolution of the fluctuations during unmixing of the systems with a reduced time scale, τ, a dimensionless time defined by[3]

$$\tau = t/t_c \tag{I-2}$$

where t is real time. The critical reduced time, τ_c, where the spinodal decomposition is described by the linearized theory with good accuracy, was shown to be a universal constant and was found to be approximately equal to 2 for some polymer systems.[4] Thus, the long characteristic time, t_c, of the systems expands the real time scale where the early stage SD occurs. Polymer systems realize beautifully this situation.[1,5,8,35]

The polymer systems to be considered in this paper have advantages of (i) a relatively narrow molecular weight distribution as they are prepared by living anionic polymerization and of (ii) being liquid well above T_g's at the measuring temperatures. Moreover, the systems can be studied in the dissipative limit where $t \gtrsim t_R/\epsilon^2$, and consequently growth of fluctuations occurs as a consequence of translational diffusion of center of mass of ~~polymer~~ molecules. Here the quantity t_R is the time required for the center of mass of the polymer chains to translate over its end-to-end distance, R_0 (called "reptation time" when the diffusion obeys the reptation mechanism[9,10]),

$$t_R \simeq R_0^2/D_c \tag{I-3}$$

and D_c is the self-diffusivity. The quantity ϵ is the thermodynamic driving force for the fluctuations to grow as defined by

$$\epsilon = (\chi - \chi_s)/\chi_s = -\frac{1}{\chi_s}\left(\frac{\partial \chi}{\partial T}\right)_{T_s}\Delta T + \mathcal{O}(\Delta T^2) \tag{I-4}$$

where χ is the thermodynamic interaction parameter between the two polymers, χ_s is the χ parameter at spinodal point, T_s is the spinodal temperature, and ΔT is the quench depth as defined by

$$\Delta T = T_s - T \tag{I-5}$$

The analyses of the early stage SD's where the linearized theory works yield the characteristic parameters[1,2,4-7,11-13] such as D_{app} and q_m, the wavenumber of the dominant mode of the fluctuations. If the constituent polymers are symmetric, having identical D_c and R_0, these parameters are given by[11]

$$D_{app} = D_c\epsilon \tag{I-6}$$

$$q_m^2 = \frac{9}{R_0^2}\epsilon \tag{I-7}$$

Thus, the ratio of the two parameters

$$q_m^2/D_{app} \sim D_c^{-1}R_0^{-2} \tag{I-8}$$

is independent of ϵ and purely depends upon the dynamical variable D_c and hence upon dynamics of the polymers at the phase transition. If the dynamics obeys reptation mode,[9,10] one finds

$$q_m^2/D_{app} \sim N^1 \tag{I-9}$$

since $D_c \sim N^{-2}$ and $R_0^2 \sim N$, where N is the polymerization index. However, if the dynamics obeys Rouse mode, one finds

† Present address: Research Center, Daicel Chemical Industries, Shinzaike, Aboshi-ku, Himeji, Hyogo 671-12, Japan.

0024-9297/87/2220-2257$01.50/0

$$q_m^2/D_{app} \sim N^0 \quad \text{(I-10)}$$

Thus, the molecular weight dependence of q_m^2/D_{app} can be a good measure to probe molecular dynamics and transport mechanism.

In this paper we investigated an early stage of SD as a function of molecular weight of one of the constituent polymers, PB, and the applicability of the linearized theory. The parameters characterizing the early stage SD will be obtained as a function of the molecular weight, from which transport mechanism of polymer chains in bulk in the ordering process at the phase transition will be discussed.

Gelles and Frank[14] also investigated the effect of molecular weight on the kinetics of phase separation in polystyrene (PS) and poly(vinyl methyl ether) blends by using the technique of excimer fluorescence. By assuming that the unmixing occurs by SD, they found the growth rate of the fluctuations to decrease with increasing PS molecular weight, but the observed effect was weaker than that expected from the scaling theory based upon reptation mechanism.[11,12,15] Objectives of our studies are along the same line as theirs, but we believe that the time-resolved light scattering analysis during the isothermal unmixing process would give much more quantitative information as to the spinodal decomposition and transport mechanism. The use of the polymers with narrow molecular weight distributions would give further advantages in our analyses on molecular dynamics.

II. Theoretical Background: Spinodal Decomposition of Asymmetric Blends

We consider here linearized theory of spinodal decomposition for the asymmetric polymer mixtures A and B with polymerization indexes N_A and N_B, statistical segment lengths a_A and a_B, self-diffusivities D_A and D_B, polymerization indexes between entanglement coupling N_{eA} and N_{eB}, and volume fraction of each component $\phi_A = \phi$ and $\phi_B = 1 - \phi$. The growth rate of the q-Fourier mode of the concentration fluctuations, $R(q)$, is given by de Gennes,[11] Pincus,[12] and Binder[13] theories

$$R(q) = \Lambda(q)q^2\left\{2\chi - \left(\frac{1}{\phi N_A} + \frac{1}{(1-\phi)N_B}\right) - \frac{a_A^2(1-\phi) + a_B^2\phi}{18\phi(1-\phi)}q^2\right\} \quad \text{(II-1)}$$

where q is the wavenumber of a particular Fourier component of the concentration fluctuations. The equation was obtained for the small q regime where $qR_{gA} \ll 1$ and $qR_{gB} \ll 1$ (R_{gK} being the gyration radius of K polymer, K = A or B) and for the time and ϵ regime where the effects of thermal fluctuating force on time evolution of scattering is negligible. In eq II-1, $\Lambda(q)$ is the Onsager kinetic coefficient describing the mutual diffusion of the two types of chains given by[11]

$$\frac{1}{\Lambda(q)} = \frac{1}{\Lambda_{AA}(q)} + \frac{1}{\Lambda_{BB}(q)} \quad \text{(II-2)}$$

where Λ_{KK} is the coefficient for the Kth polymer (K = A or B), and Λ_{KK} in the small q regime is given by[11]

$$\Lambda_{KK}(q \to 0) = D_K N_K \phi_K \quad \text{(II-3)}$$

From eq II-1 to 3, one obtains for small q regime

$$R(q) = q^2 D_{app}\left[1 - \frac{q^2}{2q_m^2}\right] \quad \text{(II-4)}$$

where

$$D_{app} = \frac{D_A D_B \bar{N}}{D_A N_A \phi_A + D_B N_B \phi_B}\epsilon \quad \text{(II-5)}$$

$$q_m^2 = \frac{9\bar{N}}{N_A N_B \bar{a}^2}\epsilon \quad \text{(II-6)}$$

$$2\chi_s = \frac{1}{\phi N_A} + \frac{1}{(1-\phi)N_B} \quad \text{(II-7)}$$

$$\bar{N} \equiv \phi N_A + (1-\phi)N_B \quad \text{(II-8)}$$

and

$$\bar{a}^2 \equiv a_A^2(1-\phi) + a_B^2\phi \quad \text{(II-9)}$$

The equations reduce to the ones derived by de Gennes[11] for the symmetric blends with $N_A = N_B = N$, $a_A = a_B = a$, and $D_A = D_B = D_C$. It is clear from eq II-5 and II-6 that the ratio q_m^2/D_{app} is independent of ϵ but depends only upon the dynamical variables and hence upon dynamics.

$$q_m^2/D_{app} = 9(D_A N_A \phi_A + D_B N_B \phi_B)/(D_A D_B N_A N_B \bar{a}^2) \quad \text{(II-10)}$$

If the diffusion occurs via reptation,[9,10]

$$D_K = D_{1K} N_{eK} N_K^{-2} \quad \text{(K = A or B)} \quad \text{(II-11)}$$

where D_{1K} is the microscopic diffusion coefficient. From eq II-10 and II-11,

$$q_m^2/D_{app} = \frac{9}{D_{1A}D_{1B}N_{eA}N_{eB}\bar{a}^2}(D_{1A}N_{eA}\phi_A N_B + D_{1B}N_{eB}\phi_B N_A) \quad \text{(for reptation)} \quad \text{(II-12)}$$

If the two polymers have identical polymerization indexes, $N = N_A = N_B$, the ratio is simply proportional to N

$$q_m^2/D_{app} \sim N \quad \text{(II-13)}$$

If the two polymers have asymmetry in the polymerization indexes but satisfy the condition

$$D_{1A}N_{eA} \simeq D_{1B}N_{eB} \equiv D_1 N_e \quad \text{(II-14)}$$

as in our experimental systems (see section V), then

$$q_m^2/D_{app} = \frac{9}{D_1 N_e \bar{a}^2}(N_B\phi_A + N_A\phi_B) \quad \text{(II-15)}$$

Comparisons of eq II-12, II-13, and II-15 clearly suggest that the mixtures with identical N_A and N_B are the most ideal and straightforward to judge the transport mechanism.

On the other hand, if the diffusion occurs in the Rouse mode

$$D_K = D_{1K} N_K^{-1} \quad \text{(II-16)}$$

then

$$q_m^2/D_{app} = 9(D_{1A}\phi_A + D_{1B}\phi_B)/(D_{1A}D_{1B}\bar{a}^2) \sim N_A^0 N_B^0 \quad \text{(II-17)}$$

III. Experimental Methods

III-1. Specimens. The samples used in this study are listed in Table I together with their number-average molecular weight, M_n, weight-average molecular weight, M_w, and heterogeneity index M_w/M_n measured by GPC. The weight fraction of styrene monomers in the SBR (designated as SBR1) was measured by using the infrared (IR) absorption at 699 cm^{-1}. The SBR sample and the PB samples (designated as PB19, PB55, PB122, and PB273) were prepared by living anionic polymerization with bu-

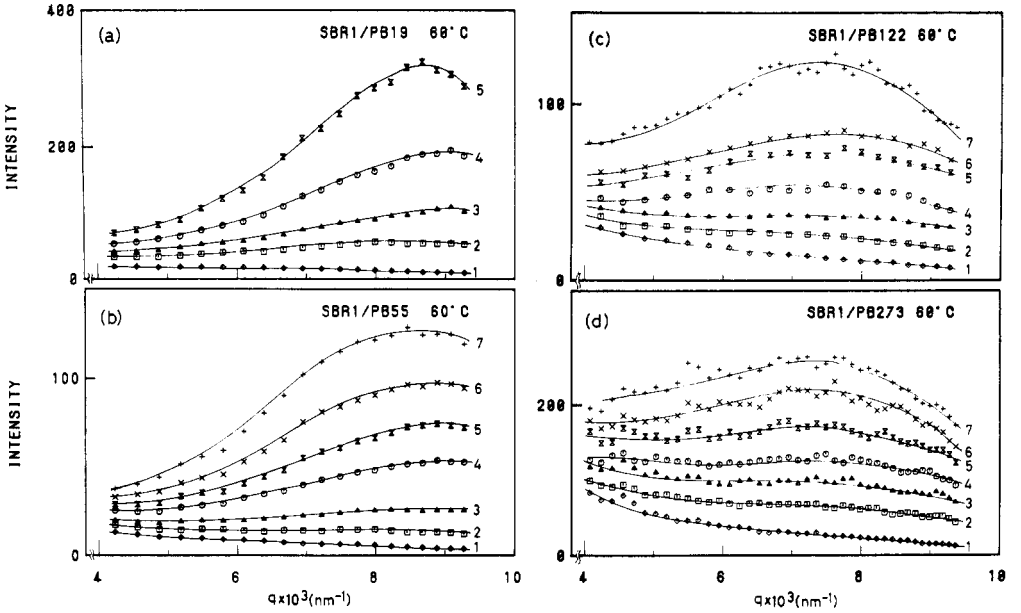

Figure 1. Time evolution of light scattering profiles during isothermal phase separation at 60 °C for the binary mixtures of (a) SBR1/PB19, (b) SBR1/PB55, (c) SBR1/PB122, and (d) SBR1/PB273. Each scattering profile was obtained at times (in minutes) after phase separation: (a) 1, 2.27; 2, 11.5; 3, 16.1; 4, 20.7; 5, 25.3; (b) 1, 2.27; 2, 11.5; 3, 20.7; 4, 29.9; 5, 34.6; 6, 39.1; 7, 43.8; (c) 1, 2.27; 2, 17.5; 3, 32.7; 4, 48.0; 5, 63.2; 6, 70.8; 7, 92.4; (d) 1, 4.69; 2, 32.7; 3, 61.2; 4, 89.7; 5, 132,4; 6, 171.6; 7, 210.9.

Table I
Characterization of Polymers Used in This Study

sample	$10^{-4}M_n$	$10^{-4}M_w$	M_w/M_n	PS, wt %	N/N_e[a]
SBR1	10.0	11.8	1.18	20	32.8
PB19	16.5	19.0	1.16	0	53.4
PB55	53.5	54.6	1.02	0	152
PB122	114	122	1.07	0	344
PB273	219	273	1.25	0	769

[a] N_e for SBR1 was measured to be 56.1 and that for PB was taken to be 35.2 from the literature.[16]

tyllithium as a catalyst and cyclohexane as the solvent.

In Table I, N and N_e are the polymerization index of entire polymer and that between entanglement coupling, respectively. The value N_e for ABR1 was determined to be

$$N_e = 56.1 \quad \text{for} \quad \text{SBR1} \tag{III-1}$$

by rheology measurement by using the relationship

$$G_{eN}^0 \simeq 3.56 G_{max}'' = \rho RT/M_e \tag{III-2}$$

where G_{eN}^0 is the equilibrium plateau modulus, G_{max}'' is the maximum loss modulus with respect to frequency at a given temperature, T, ρ is the mass density, R is the gas constant, and M_e is the molecular weight between the entanglements. The value G_{max}'' was 1.56×10^6 dyn/cm^2 at 323 K, and ρ was 0.92 g/cm^3, from which M_e was estimated to be 4.5×10^3 and N_e to be 56.1. The value N_e for PB was taken from Ferry's book[16] to be 35.2 by finding the value for PB sample having microstructure close to our PB.

The fractions of cis, trans, and vinyl linkages of the butadiene part were measured by IR. They are, respectively, 0.16, 0.23, and 0.61 for SBR1 and 0.19, 0.35, and 0.46 for PB19. The microstructure for other PB's (PB55, PB122, and PB273) should be similar to that for PB19.

III-2. Preparation of the Mixtures. Mixtures of SBR1/PB19, SBR1/PB55, SBR1/PB122, and SBR1/PB273 were prepared as follows. All the mixtures studied were 50/50 wt/wt, and they were dissolved in 7 wt % toluene solution. Toluene is a neutrally good solvent for PB and SBR. The solution containing 7 wt % total amount of polymer was homogeneous and was cast into film specimens by slowly evaporating the solvent. The solvent was completely evaporated until a constant weight was attained.

The films thus obtained were further mechanically mixed by holding and pressing repeatedly (typically 30 times) in order to make "*homogenized films*" immediately before the use for the studies of the phase separation kinetics. Significance of the *mechanical mixing or homogenization* was discussed in previous papers[1,17] and will be discussed extensively in a forthcoming paper.[18] Light scattering studies on the homogenized films showed that the homogenization brings the mixtures to a state corresponding to the single phase region near the spinodal point.[18]

III-3. Time-Resolved Light Scattering Technique. Isothermal unmixing process from the homogenized mixtures was analyzed in real time and in situ with an automated laser-light scattering photometer constructed in our laboratory.[5] The photometer utilizes a photomultiplier with a rapid step-scanning device with data acquisition into microcomputer as a function of time during the unmixing process. Further details of the apparatus were described elsewhere.[5]

IV. Experimental Results and Discussions

IV-1. Time Evolution of Light Scattered Intensity $I(q, t)$. Figure 1 shows typical time evolution of light scattering profiles during isothermal phase separation at 60 °C from the homogenized mixtures of (a) SBR1/PB19, (b) SBR1/PB55, (c) SBR1/PB122, and (d) SBR1/PB273 where some but not all of the time-sliced profiles only in the early stage unmixing process were shown. The ordinate in each figure is relative intensity so that the intensity level can be compared only within each figure but not between different figures. The abscissa is the scattering vector, q, defined by

$$q = (4\pi/\lambda) \sin(\theta/2) \tag{IV-1}$$

where λ and θ are the wavelength of light in the medium and the scattering angle in the medium, respectively. It should be noted that the scattered intensity at the scattering vector, q, is related to the intensity of the q-Fourier

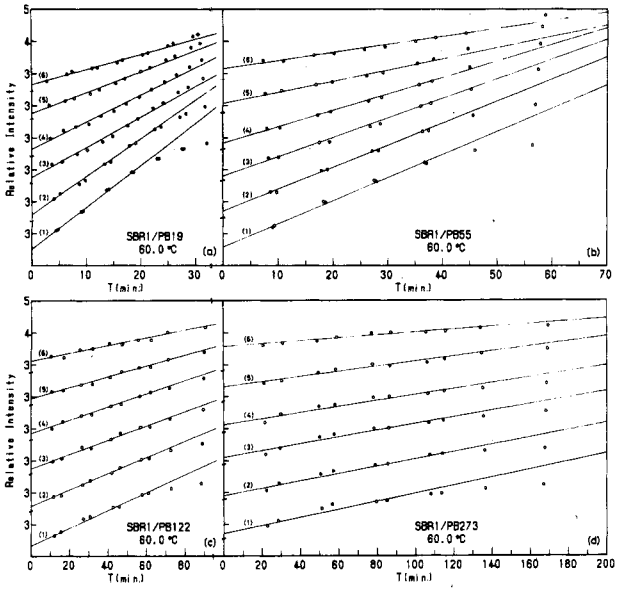

Figure 2. Time evolution of light scattering intensity at various q's during the isothermal phase separation at 60 °C for the binary mixtures of (a) SBR1/PB19, (b) SBR1/PB55, (c) SBR1/PB122, and (d) SBR1/PB273. The logarithm of the intensity was plotted as a function of time t (min). Curves 1–6 were obtained at q = 9.08×10^{-3}, 8.23×10^{-3}, 7.22×10^{-3}, 6.39×10^{-3}, 5.50×10^{-3}, and 4.24×10^{-3} nm^{-1}, respectively.

component of the fluctuations.

Each mixture gives rise to similar time-evolution behavior of scattering: increase of scattered intensity and appearance of the scattering maximum at the high q region covered in this experiment. The q value at which the scattered intensity reaches maximum, q_m, appears to be independent of time in the early stage unmixing process for each mixture,

$$q_m(t) = q_m(0)t^0 \qquad \text{(IV-2)}$$

Comparisons of Figures 1 and 2 will reveal that the early stage of unmixing process can be described with good accuracy by the linearized theory of SD and that the profiles 1–4 in Figure 1a, 1–6 in Figure 1b, 1–5 in Figure 1c, and 1–5 in Figure 1d should correspond to the linear SD regime. The behavior given by eq IV-2 may be clearly seen for the mixtures having higher molecular weights (e.g., parts b–d of Figure 1). The values $q_m(0)$ appear to decrease with increasing the molecular weight, so that the wavelength, Λ_m, of the dominant mode of concentration fluctuations increases with increasing molecular weight. Moreover, the larger the molecular weight, the longer the time limit defined as t_{max} where the linear SD behavior is observed. In other words, the larger the molecular weight, the slower the spinodal decomposition rate.

The rates of SD and t_{max} may be more quantitatively investigated in Figure 2, where logarithms of relative scattered intensity, $I(q, t)$, were plotted as a function of time, t, after initiation of isothermal unmixing at 60 °C for each mixture (a) for SBR1/PB19, (b) for SBR1/PB55, (c) for SBR/PB122, and (d) for SBR/PB273. Each plot shows ln $I(q, t)$ vs. t at the same q values (but not all q values measured in this experiments); curves 1–6 for each mixture were obtained, respectively, at q values of 9.08×10^{-3}, 8.23×10^{-3}, 7.22×10^{-3}, 6.39×10^{-3}, 5.50×10^{-3}, and 4.24×10^{-3} nm^{-1}.

Each figure shows clearly that, in the early stage unmixing process, ln $I(q, t)$ at a given q linearly increases with t, indicating the exponential growth of the concentration fluctuations of all q-Fourier modes and of the associated

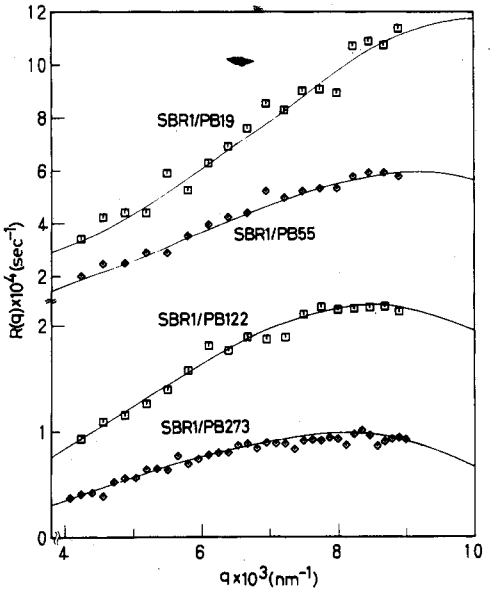

Figure 3. Growth rate $R(q)$ as a function of q at 60 °C for the binary mixtures.

scattered intensity for the q range covered in this experiment,

$$I(q, t) = I(q, 0) \exp[2R(q)t] \qquad \text{(IV-3)}$$

$$S(q, t) = S(q, 0) \exp[R(q)t] \qquad \text{(IV-4)}$$

where $S(q, t)$ is the time evolution of order parameter conjugated with the scattered intensity,

$$I(q, t) = \langle |S(q, t)|^2 \rangle_T \qquad \text{(IV-5)}$$

where $\langle\ \rangle_T$ denotes the average over all possible probability distributions of the order parameter. The observations given by eq IV-2–IV-4 strongly suggest that the unmixing behavior is approximated by the linearized theory of SD, as reported also for other polymer systems.[1,4,8,19,20]

From the slope of each straight line, one can determine the growth rate, $R(q)$, for each mixture. Comparisons of the time evolution behavior of the scattered intensity for the mixtures shown in Figure 2 clearly indicate that $R(q)$ and t_{max} strongly depend on molecular weight. The larger the molecular weight, the slower the growth, i.e., the smaller the value of $R(q)$ and the larger the value of t_{max}.

It should be pointed out that in the later stage of unmixing (e.g., in the time scale of $t > 30$ min in Figure 2a, $t > 60$ min in Figure 2b, $t > 90$ min in Figure 2c, and $t > 125$ min in Figure 2d), the intensity increase with time deviates from the exponential behavior at all q's due to the onset of various coarsening mechanisms.[4,21-31] In the later stage the growth rates become much slower than that of the exponential behavior as predicted by eq IV-3, the data points thus falling below the straight lines at all q's. The deviations of the data points in the time scale of $25 \lesssim t \lesssim 30$ min in Figure 2a and $45 \lesssim t \lesssim 60$ min in Figure 2b, for example, are not yet those as described above. The upward deviation at small q's from the straight line and the downward deviations at large q's from the straight line in that time scale may be due to the effect of thermal fluctuating force as described by Okada and Han;[8] brief discussions related to this point will be given in section IV-3. In the larger time scale, the deviations from the straight lines occur always downward at all q's. The analyses in these late stage unmixing processes are given elsewhere.[4,23,32]

IV-2. Growth Rate for q-Fourier Mode of Fluctuations. Figure 3 shows the growth rates, $R(q)$, as a

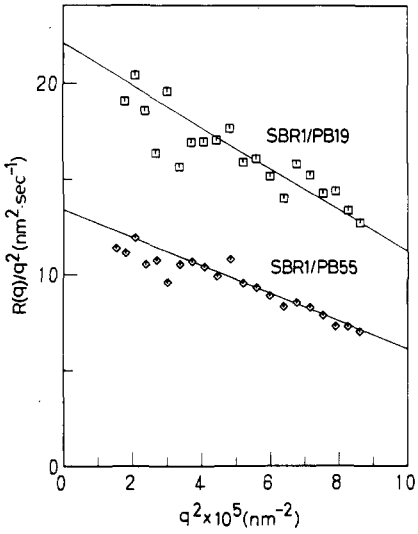

Figure 4. Plots of $R(q)/q^2$ vs. q^2 at 60 °C for the binary mixtures of SBR1/PB19 and SBR1/PB55.

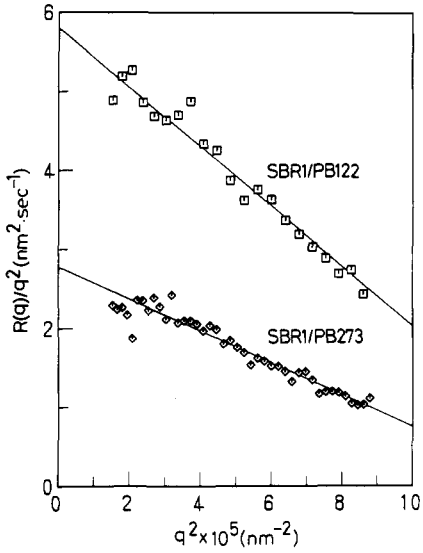

Figure 5. Plots of $R(q)/q^2$ vs. q^2 at 60 °C for the binary mixtures of SBR1/PB122 and SBR1/PB273.

function of q for the four mixtures with different molecular weights as determined from the analyses shown in Figure 2. The growth rates, $R(q)$, for all q-Fourier modes covered in this study decrease with increasing molecular weights of the mixtures. The q dependence of $R(q)$ has a functional form as given by eq II-4, the curves drawn by the solid lines being the best-fitted results of the experimental $R(q)$ with eq II-4. It should be noted that the best-fitted curves give also the straight lines in the plots as shown in Figures 4 and 5. The growth rates, $R(q)$, for the mixtures appear to have a maximum R_m at $q = q_m$. The growth rate, R_m, and the wavenumber, q_m, of the dominant mode of the concentration fluctuations seem to depend strongly and moderately upon the molecular weight of the mixture, respectively. The larger the molecular weight, the smaller the values R_m and q_m.

IV-3. Test of Linearized Theory of Spinodal Decomposition. Figures 4 and 5 show the plots of $R(q)/q^2$ vs. q^2 for the four mixtures which provide a critical test of eq II-4 obtained by the linearized theory of SD. All the experimental results seem to exhibit, with good accuracy, the linearity as predicted by eq II-4. This evidence together with the evidence given by eq IV-2 and IV-3 suggests that the linearized theory of SD describes the early stage unmixing behavior of the real systems with good approximation over the q range covered in this study. In the previous paper,[1] the mixture SBR1/PB19 was found to have $T_s \simeq 400$ °C. Hence, the phase separation at 60 °C corresponds to the phase separation under apparently large quench depth. It will be shown later in section VI that the "effective quench depth" is not as large as the actual quench depth appears to be.

The thermal fluctuation force[33] is one physical factor which causes the deviation from behavior as predicted by the linearized theory of SD. Its effect is especially important at high q's near q_c where $R(q = q_c) = 0$

$$q_c^2 = 2q_m^2 \qquad \text{(IV-6)}$$

Unfortunately our light scattering technique cannot cover the high q regime of $q \simeq q_c$ but can only cover the low q regime satisfying $q \ll q_m$. Hence, we are observing the q regime where the effects of thermal fluctuating force are relatively weak. Even in small q regime, the effects should be detected if the effective quench depth is small enough.[13,33,38] In fact, Okada and Han[8] observed the effects clearly for quench depths as large as 0.29 °C but not for quench depths as large as 0.44 °C for their polymer mixtures composed of polystyrene and poly(vinyl methyl ether). In our earlier paper,[4] we analyzed the effects of thermal fluctuation force on the time evolution of scattered intensity at small q and found that the effects are greater for the mixtures with larger molecular weights under a given ϵ. Under a given ϵ, the effects are greater in polymer mixtures than in small molecular fluids by a factor of N (degree of polymerization),[4] which may be a possible reason why the effects were observed at the large quench depth, ΔT, of 0.29 °C in the studies of Okada and Han,[8] much larger than those normally employed in the small molecular fluids (ΔT of the order of 10^{-3} °C being employed). For a given N, the effects decrease with increasing ϵ, as is well-known from earlier studies.[8,13,33,38] The "effective quench depths" or ϵ's of our systems are much larger than 0.29 °C, and hence the effects would hardly be seen or be small, if they exist, in the small q regime for our system. This factor appears to act in favor of the linearized theory of SD.

The plots of Figures 4 and 5 will yield the parameters characterizing the early stage SD such as D_{app} and q_m or R_m and Λ_m as defined by

$$R_m = R(q_m(0)) \qquad \text{(IV-7)}$$

and

$$\Lambda_m = 2\pi/q_m(0) \qquad \text{(IV-8)}$$

The quantities R_m and Λ_m are the maximum growth rate of the fluctuations and the wavelength of the dominant mode of the fluctuations. The parameters thus estimated are summarized in Table II. In Table II, parameter τ_m is defined by

$$\tau_m = R_m^{-1} \qquad \text{(IV-9)}$$

and t_c is the characteristic time of the mixture as defined by eq I-1, where ξ is given by

$$\xi = q_m(0)^{-1} \qquad \text{(IV-10)}$$

IV-4. Parameters Characterizing Early Stage of Spinodal Decomposition. The apparent or mutual diffusivity, D_{app}, and the wavenumber, $q_m(0)$, of the dominant mode of the fluctuations decrease with increasing molecular weight of one component, e.g., PB (see Table II). The value of D_{app} depends both upon ϵ, the thermodynamic driving force which depends on N_K at a given

Table II
Parameters Characterizing Early Stage of Spinodal Decomposition at 60 °C

sample	D_{app},[a] nm^2/s	10^4R_m,[b] s^{-1}	$10^3q_m(0)$,[c] nm^{-1}	$10^{-2}\Lambda_m$,[d] nm	$10^{-3}\tau_m$,[e] s	$10^{-3}t_c$,[f] s
SBR1/PB19	22	11	10	6.3	0.92	0.46
SBR1/PB55	13	6.0	9.5	6.7	1.7	0.84
SBR1/PB122	5.8	2.2	8.8	7.2	4.6	2.3
SBR1/PB273	2.8	0.96	8.4	7.5	10	5.2

[a] Equation II-4. [b] Equation IV-7. [c] Equation IV-2. [d] Equation IV-8. [e] Equation IV-9. [f] Equations I-1 and IV-10.

Table III
Parameters Characterizing Early Stage of Spinodal Decomposition at 60 °C

sample	$10^6(q_m^2/D_{app})$, s/nm^4	$10^{-3}t_{max}$, s	τ_c	$\Lambda_m/R_{g,PB}$	$R_{g,PB}$, nm
SBR1/PB19	4.4	1.2	2.4	35	18
SBR1/PB55	6.7	2.1	2.5	21	31
SBR1/PB122	13	4.2	1.8	16	46
SBR1/PB273	26	7.2	1.4	11	70

temperature, and D_K, the transport terms which depend also on N_K (see eq II-5). Similarly $q_m(0)$ depends upon ϵ and chain dimension R_{gK} which also depends upon N_K. Generally N dependences of D_{app} and $q_m(0)$ are a consequence of N dependences of D_K, R_{gK}, and ϵ. From eq II-7, the value χ_s for our mixtures is given by

$$\chi_s \simeq \frac{1}{N_{PB}} + \frac{1}{N_{SBR}} \qquad \text{(IV-11)}$$

simply because $\phi \simeq {}^1/_2$, where N_{PB} and N_{SBR} are the polymerization indexes for PB and SBR, respectively. Now that the decrease of χ_s with increasing N_{PB} given by

$$-d\chi_s/dN_{PB} = N_{PB}^{-2} \qquad \text{(IV-12)}$$

is small for large N_{PB}, the increase of ϵ with increasing N_{PB} is also expected to be small. Hence, the N dependences of D_{app} and $q_m(0)$ may primarily be determined by those of D_K and R_{gK}. Since D_{app}/ϵ and q_m^2/ϵ are expected to decrease with increasing N_{PB}, the trends found in the experiments appear to be justified by the mean field predictions given by eq II-4–II-6. Likewise the N dependences of other parameters also should primarily be determined by the N dependences of R_{gK} and D_K rather than that of ϵ.

It is interesting to note that the characteristic time, t_c, increases by about 10 times, from about 500 to 5000 s, by increasing N_{PB}. A similar increase of the relaxation time, τ_m (from about 900 to 10 000 s), for the dominant mode of fluctuations to grow was also found. The wavelength of the dominant mode of fluctuations, Λ_m, seems to be much larger than the molecular sizes themselves, R_{gK}'s, by 1 order of magnitude for all the mixtures (i.e., $\Lambda_m/R_{gK} \simeq 10$), a possible interpretation of which will be given in section VI.

IV-5. τ_c. In previous papers,[1,4] we indicated that the critical reduce time, τ_c, below which the unmixing behavior can be approximated by the linearized theory of SD, is a universal constant[4] approximately equal to 2.

$$\tau_c = t_{max}/t_c \simeq 2$$

The universality was tested also for the mixtures studied here. The t_{max}'s were estimated to be 1.2×10^3, 2.1×10^3, 4.2×10^3, and 7.2×10^3 s for SBR1/PB19, SBR1/PB55, SBR1/PB122, and SBR1/PB273, respectively, from the plots as shown in Figure 2 (see Table III). For SBR1/PB19 and SBR1/PB55, t_{max}'s were determined at the highest accessible q's, which are still slightly smaller than the corresponding q_m's, but for SBR1/PB122 and SBR10PB273, they were determined at corresponding q_m's. The estimated values of τ_c are also included in Table III.

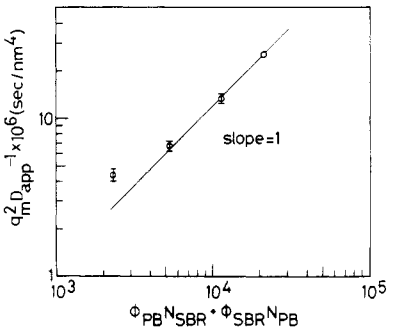

Figure 6. Plot of q_m^2/D_{app} as a function of the effective polymerization index, $\phi_{PB}N_{SBR} + \phi_{SBR}N_{PB}$. If the mutual diffusion occurs through reptation, a slope of 1 should be observed.

The results approximately assure the relationship of $\tau_c \simeq 2$.

V. Transport Mechanism

As already discussed in section II, the ratio q_m^2/D_{app} is a good probe to investigate the dynamics and transport mechanism of polymer molecules in the mixtures undergoing the phase transition. The ratios were listed in Table III and plotted in Figure 6 as a function of the effective polymerization index, N_{eff}

$$N_{eff} \equiv \phi_{PB}N_{SBR} + (1 - \phi_{PB})N_{PB} \qquad \text{(V-1)}$$

where ϕ_{PB} is the volume fraction of PB in the mixture of PB and SBR. As is clearly seen from Figure 6, the experimental results obtained at the three mixtures with larger molecular weights tend to support N_{eff}^1,

$$q_m^2/D_{app} \sim N_{eff}^1 \qquad \text{(V-2)}$$

and hence the reptation mechanism. In these three mixtures, N/N_e for SBR is about 33 and N/N_e for PB is from about 150 to 770 (Table I). However, for the mixture with the smallest molecular weight (SBR1/PB19), there is a deviation from the behavior as given by eq V-2.

Uncertainty of our conclusion results from inequality of N_{SBR} and N_{PB} which involves detailed information of $D_{1A}N_{eA}$ and $D_{1B}N_{eB}$ as is obvious from eq II-12. Further investigations along this line which use SBR and PB specimens having about equal N_{PB} and N_{SBR} are in progress. Before closing this section, we will make a rough estimation on accuracy of our assumption of eq II-14 or a ratio of $(N_e/\zeta)_{SBR}$ to $(N_e/\zeta)_{PB}$ where ζ_K is the monomeric friction coefficient of K (K = SBR or PB).

From Table 12-III of Ferry's book,[16] one can estimate monomeric friction coefficients, ζ_{SBR} and ζ_{PB}, at 60 °C by using the WLF equation.[16] For example, SBR has the values for log ζ (dyn·s/cm) of −6.11, −7.93, and −8.25 at 298, 373, and 398 K, respectively, from which one obtains constants C_1 and C_2 in the WLF equation

$$\log\left(\frac{\zeta_0 T_0}{\zeta T}\right)_{SBR} = \frac{C_1(T - T_0)}{C_2 + T - T_0} \qquad \text{(V-3)}$$

where T_0 is the reference temperature (298 K) and ζ_0 is ζ at 298 K

$$C_1 = 4.07 \quad \text{and} \quad C_2 = 102.4 \qquad \text{(V-4)}$$

Hence, one can estimate ζ_{SBR} at 60 °C (=333 K) as

$$\zeta_{SBR} = 6.31 \times 10^{-8} \quad \text{dyn·s/cm} \qquad \text{(V-5)}$$

Similarly by use of the tabulated values for poly-1,4-butadiene in Table 12-III of Ferry's book,[16] C_1 and C_2 for PB can be estimated as

$$C_1 = 3.15 \quad \text{and} \quad C_2 = 176.5 \qquad \text{(V-6)}$$

for $T_0 = 298$ K, from which one can estimate ζ_{PB} at 60 °C as

$$\zeta_{PB} = 4.79 \times 10^{-8} \quad \text{dyn·s/cm} \qquad \text{(V-7)}$$

It should be noted that the microstructure for poly-1,4-butadiene in Table 12-III is different from that of our PB; hence, ζ_{PB} for our PB is not necessarily the same as that given by eq V-7. However, the value of ζ_{PB} given by eq V-7 should be much closer to ζ_{PB} for our PB than that expected for poly-1,2-butadiene. Thus, we use the value given by eq V-7 for our PB. The value of $(N_e)_{SBR}$ measured was 56.1 and that taken from Table 13-I of Ferry's book[16] was 45.8. The value of $(N_e)_{PB}$ was 35.2 from Table 13-I. By using these values, one can estimate the ratio

$$(D_1N_e)_{SBR}:(D_1N_e)_{PB} = (N_e/\zeta)_{SBR}:(N_e/\zeta)_{PB} = 1:1.02 \text{ or } 1.14:1 \qquad \text{(V-8)}$$

by using $(N_e)_{SBR} = 45.8$ or 56.1, respectively. Thus, the assumption of eq II-14 and hence eq II-15 may be assured.

VI. Interpretation of Small q_m or Large Λ_m for the Dominant Mode of Fluctuations

We now give an interpretation of large Λ_m's for the wavelength of the dominant mode of the fluctuation in the early stage. From Table II, Λ_m's vary from 630 to 750 nm upon increasing molecular weight of PB, which appear to be quite large compared with the gyration radius of the component polymer, e.g., PB denoted here as $R_{g,PB}$. Table III contains $R_{g,PB}$ (unperturbed radius of gyration) and $\Lambda_m/R_{g,PB}$. The ratios $\Lambda_m/R_{g,PB}$ appear to be large, changing from 35 to 11 with increasing molecular weight of PB.

From eq II-6 and IV-8, it follows that

$$\Lambda_m = \frac{2\pi}{3}\left(\frac{N_A^{1/2}N_B^{1/2}(\bar{a}^2)^{1/2}}{\bar{N}^{1/2}}\right)\epsilon^{-1/2} \qquad \text{(VI-1)}$$

and

$$\frac{\Lambda_m}{R_{g,A}} = \frac{2\pi 6^{1/2}}{3}\left(\frac{N_B^{1/2}(\bar{a}^2)^{1/2}}{\bar{N}^{1/2}a_A}\right)\epsilon^{-1/2} \qquad \text{(VI-2)}$$

Hence, Λ_m and $\Lambda_m/R_{g,A}$ can be, in principle, very large when the mixture is close to spinodal point. The spinodal temperature for the mixture SBR1/PB19 (70/30 v/v) was previously determined[1] by measuring $q_m^2(0)$ as a function of temperature and by extrapolating the value $q_m^2(0)$ to zero and finding the temperature T_s at which $q_m^2(0) = 0$. The extrapolation method uses eq I-4 and II-6, hence, a mean field relation of $q_m^2(0) \sim \Delta T$. The value of T_s thus estimated was $\simeq 400$ °C. Thus, *actual quench depth* is very large, $\Delta T = 400 - 60 = 340$ °C, yet $\Lambda_m/R_{g,PB}$ is very large, which appears to be puzzling at first glance and is a subject of present discussions. It may be quite obvious from eq VI-1, VI-2, and I-4 that a key to understanding the physics is temperature dependence of χ.

It should be noted that the thermodynamic interaction parameter between SBR and PB ($\chi_{PB/SBR}$) is much smaller than that between PS (polystyrene) and PB ($\chi_{PB/PS}$), because of incorporation of butadiene monomers in SBR. If

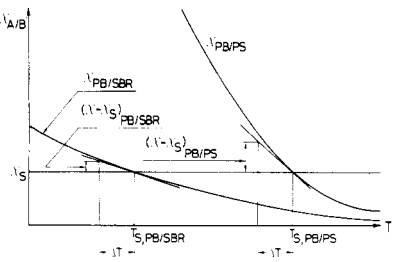

Figure 7. Schematic illustration of temperature dependence of χ values for binary mixtures of PB/PS and PB/SBR. Note that the small temperature dependence of χ for PB/SBR results in small "effective quench depth, ϵ", even under the given large quench depth, ΔT.

the fraction of butadiene in SBR is defined as ψ, then one can show the following relationship by a simple thermodynamic consideration[36] or by using random phase approximation:[15,34]

$$\chi_{PB/SBR} = (1 - \psi)^2\chi_{PB/PS} \qquad \text{(VI-3)}$$

Now that SBR has $\psi = 0.8$, $(1 - \psi)^2 = 0.04$ and hence $\chi_{PB/SBR}$ is very small compared with $\chi_{PB/PS}$ for the PB/PS mixture with polymerization indexes identical with those of PB/SBR, as schematically shown in Figure 7. Likewise the temperature dependence of $\chi_{PB/SBR}$ should be very small compared with that of $\chi_{PB/PS}$. Hence,

$$(\chi - \chi_s)_{PB/SBR} \simeq -\left(\frac{\partial\chi}{\partial T}\right)_{T_{s,PB/SBR}}\Delta T \qquad \text{(VI-4)}$$

$$(\chi - \chi_s)_{PB/SBR} \simeq -(1 - \psi)^2\left(\frac{\partial\chi}{\partial T}\right)_{T_{s,PB/PS}}\Delta T \qquad \text{(VI-5)}$$

and

$$(\chi - \chi_s)_{PB/PS} \simeq -\left(\frac{\partial\chi}{\partial T}\right)_{T_{s,PB/PS}}\Delta T \qquad \text{(VI-6)}$$

Comparison between eq IV-5 and IV-6 elucidates that in the mixture of PB/SBR, the *effective quench depth*, $(1 - \psi)^2\Delta T$, can be very small and the mixture can be close to the spinodal point, $T_{s,PB/SBR}$, even in the case when the actual quench depth, ΔT, is very large. The quench depth of 1 °C for PB/PS corresponds to that of 0.04 °C for PB/SBR, and hence PB/SBR is *effectively close to criticality*, which again is schematically shown in Figure 7 and which is a key physical factor to account for the large Λ_m and $\Lambda_m/R_{g,PB}$ in Tables II and III, respectively.

From eq VI-2, it follows that

$$(\Lambda_m/R_{g,PB})_{PB/SBR} = K_{PB/SBR}\epsilon_{PB/SBR}^{-1/2} \qquad \text{(VI-7)}$$

$$(\Lambda_m/R_{g,PB})_{PB/PS} = K_{PB/PS}\epsilon_{PB/PS}^{-1/2} \qquad \text{(VI-8)}$$

We compare the ratios for the two mixtures PB/SBR and PB/PS having corresponding polymerization indexes of the constituent polymers, and at identical quench depths, then

$$\left(\frac{\Lambda_m}{R_{g,PB}}\right)_{PB/SBR}\Big/\left(\frac{\Lambda_m}{R_{g,PB}}\right)_{PS/PB} = K\left(\frac{\epsilon_{PB/SBR}}{\epsilon_{PB/PS}}\right)^{-1/2} = K\left\{\frac{(\chi - \chi_s)_{PB/SBR}}{(\chi - \chi_s)_{PB/PS}}\right\}^{-1/2} = K(1 - \psi)^{-1} \qquad \text{(VI-9)}$$

where K is the numerical factor of order unity. Thus, $(\Lambda_m/R_{g,PB})_{PB/SBR}$ can be larger than $(\Lambda_m/R_{g,PB})_{PB/PS}$ by a factor of $(1 - \psi)^{-1}$, i.e., by a factor of about 5 for our system.

Further detailed discussions on the values of $(\Lambda_m/R_{g,PB})_{PB/SBR}$ in comparison with the theoretical values will be given in the Appendix.

Acknowledgment. We are grateful to Research and Development Laboratory, Japan Synthetic Rubber Co., Ltd., Yokkaichi, Mie 510, Japan, for their help in preparing the experimental samples of PB and SBR used in this work.

Appendix. Comparison of Experimental and Theoretical $\Lambda_m/R_{g,PB}$ for PB/SBR Mixtures

We compare the theoretical values of $\Lambda_m/R_{g,PB}$ determined from eq VI-2 and the experimental values shown in Table III in order to investigate whether the experimental values can be predicted from the mean field theory.

Experimental data on the temperature dependence of $\chi_{PB/SBR}$ for the PB/SBR mixture are not available. We estimate it from the temperature dependence of $\chi_{PB/PS}$[37] by using eq VI-3,

$$\chi_{PB/PS} = -0.0046 + 30.4/T \quad \text{(A1)}$$

Equation A1 was determined from temperature dependence of small-angle X-ray scattering profile from polystyrene–polybutadiene block polymer in disordered state. From eq A1 and VI-5 and by using $\psi = 0.8$, it follows that

$$(\chi - \chi_s)_{PB/SBR} = \frac{1.22}{T_{s,PB/PS}^2}\Delta T \quad \text{(A2)}$$

We further calculate $(\chi - \chi_s)_{PB/SBR}$ and ϵ for a particular mixture, SBR1/PB19, from eq IV-11,

$$\chi_s = \frac{1}{1840} + \frac{1}{3510} = 8.28 \times 10^{-4} \quad \text{(A3)}$$

The spinodal temperature $T_{s,PB/PS}$ can be estimated from eq A1 and A3 to be 5.6×10^3 K, from which $(\chi - \chi_s)_{PB/SBR}$ can be estimated as

$$(\chi - \chi_s)_{PB/SBR} = 3.88 \times 10^{-8}\Delta T \quad \text{(A4)}$$

Hence, ϵ is given by

$$\epsilon = 4.67 \times 10^{-5}\Delta T \quad \text{(A5)}$$

for SBR1/PB19. One should note that the coefficient $\epsilon/\Delta T$ is very small. From eq A5 and VI-2, the theoretical value of $(\Lambda_m/R_{g,PB})_{theor.}$ can be estimated by using $\Delta T = 400 - 60 = 340$ K,

$$\left(\frac{\Lambda_m}{R_{g,PB}}\right)_{theor} = \frac{2\pi 6^{1/2}}{3}\frac{(1840)^{1/2}}{0.5(1840)^{1/2} + 0.5(3510)^{1/2}}(0.016)^{-1/2} = 34 \quad \text{(A6)}$$

where $a_{SBR} = a_{PB}$ is assumed. The theoretical value turns out to be quite close to the experimental value of 35 (see Table III). Consequently the large experimental value of $\Lambda_m/R_{g,PB}$ is interpreted as a consequence of the small temperature coefficient of ϵ.

Registry No. PB, 9003-17-2; SBR, 9003-55-8.

References and Notes

(1) Part 1 of this series: Izumitani, T.; Hashimoto, T. *J. Chem. Phys.* **1985**, *83*, 3694.
(2) Cahn, J. W. *J. Chem. Phys.* **1965**, *42*, 93.
(3) Chou, Y. C.; Goldburg, W. I. *Phys. Rev. A* **1979**, *23*, 2105.
(4) Hashimoto, T.; Itakura, M.; Shimizu, N. *J. Chem. Phys.* **1986**, *85*, 6773.
(5) Hashimoto, T.; Kumaki, J.; Kawai, H. *Macromolecules* **1983**, *16*, 641.
(6) Snyder, H. L.; Meakin, P.; Reich, S. *Macromolecules* **1983**, *16*, 757.
(7) Hashimoto, T. In *Current Topics in Polymer Science-1984*; Ottenbrite, R. M., Utracki, L. A., Inoue, S., Eds.; Hanser: New York, 1987; Vol. 2, pp 197–242.
(8) Okada, M.; Han, C. *J. Chem. Phys.* **1986**, *85*, 5317.
(9) de Gennes, P. G. *J. Chem. Phys.* **1971**, *55*, 572.
(10) Doi, M.; Edwards, S. F. *J. Chem. Soc., Faraday Trans. 2* **1978**, *74*, 1789, 1802, 1818.
(11) de Gennes, P. G. *J. Chem. Phys.* **1980**, *72*, 4756.
(12) Pincus, P. *J. Chem. Phys.* **1981**, *75*, 1996.
(13) Binder, K. *J. Chem. Phys.* **1983**, *79*, 6387.
(14) Gelles, R.; Frank, C. W. *Macromolecules* **1983**, *16*, 1448.
(15) de Gennes, P. G. *Scaling Concept in Polymer Physics*; Cornell University Press: Ithaca, NY, and London, 1979.
(16) Ferry, J. D. *Viscoelastic Properties of Polymers*, 3rd ed.; Wiley: New York, 1980; p 374, Table 13-I.
(17) Hashimoto, T.; Izumitani, T. *Polym. Prepr., Am. Chem. Soc., Div. Polym. Chem.* **1985**, *26*, 66.
(18) Hashimoto, T.; Izumitani, T.; Takenaka, M., to be submitted to *Macromolecules*.
(19) Hashimoto, T.; Sasaki, K.; Kawai, H. *Macromolecules* **1984**, *17*, 2812.
(20) Sasaki, K.; Hashimoto, T. *Macromolecules* **1984**, *17*, 2818.
(21) McMaster, L. P. In *Copolymers, Polyblends and Composites*; Platzer, N. A., Ed.; Advances in Chemistry Series 142; American Chemical Society: Washington, DC, 1975; p 43.
(22) Snyder, H. L.; Meakin, P. *J. Chem. Phys.* **1983**, *79*, 5588.
(23) Hashimoto, T.; Itakura, M.; Hasegawa, H. *J. Chem. Phys.* **1986**, *85*, 6118.
(24) Yang, H.; Shibayama, M.; Stein, R. S.; Shimidzu, N.; Hashimoto, T. *Macromolecules* **1986**, *19*, 1667.
(25) Langer, J. S.; Baron, M.; Miller, H. D. *Phys. Rev. A* **1975**, *11*, 1417.
(26) Kawasaki, K. In *Phase Transitions and Critical Phenomena*; Domb, C., Green, M. S., Eds.; Academic: London, 1972; Vol. 2.
(27) Kawasaki, K.; Ohta, T. *Prog. Theor. Phys.* **1978**, *59*, 362.
(28) Lifshitz, I. M.; Slyozov, V. V. *J. Phys. Chem. Solids* **1961**, *19*, 35.
(29) Binder, K.; Staufer, D. *Phys. Rev. Lett.* **1974**, *33*, 1006. Binder, K. *Phys. Rev. B* **1977**, *15*, 4425.
(30) Furukawa, H. *Phys. Lett. A* **1983**, *98*, 28; *Adv. Phys.* **1985**, *34*, 703.
(31) Siggia, E. D. *Phys. Rev. A* **1979**, *20*, 595.
(32) Izumitani, T.; Takenaka, M.; Hashimoto, T., unpublished results.
(33) Cook, H. E. *Acta Metall.* **1970**, *18*, 297.
(34) Mori, K.; Tanaka, H.; Hashimoto, T. *Macromolecules* **1987**, *20*, 381.
(35) Hill, R. G.; Tomlins, P. E.; Higgins, J. S. *Macromolecules* **1985**, *18*, 2555.
(36) Roe, R. J.; Zin, C. W. *Macromolecules* **1980**, *13*, 1221.
(37) Mori, K.; Okawara, A.; Hashimoto, T., unpublished results.
(38) Strobl, G. R. *Macromolecules* **1985**, *18*, 558.